

**EVALUATING LIVING SHORELINE PERFORMANCE AND VESSEL  
WAKE USING THE SHIP WAKE MODULE OF FUNWAVE-TVD**

by

Oscar Williams

A thesis submitted to the Faculty of the University of Delaware in partial fulfillment of the requirements for the degree of Master of Science in Civil Engineering.

Summer 2022

© 2022 Oscar Williams  
All Rights Reserved

**EVALUATING LIVING SHORELINE PERFORMANCE AND VESSEL  
WAKE USING THE SHIP WAKE MODULE OF FUNWAVE-TVD**

by

Oscar Williams

Approved: \_\_\_\_\_  
Jack A. Puleo, Ph.D.  
Professor in charge of thesis on behalf of the Advisory Committee

Approved: \_\_\_\_\_  
Jack A. Puleo, Ph.D.  
Chair of the Department of Civil Engineering

Approved: \_\_\_\_\_  
Levi T. Thompson, Ph.D.  
Dean of the College of Engineering

Approved: \_\_\_\_\_  
Louis F. Rossi, Ph.D.  
Vice Provost for Graduate and Professional Education and  
Dean of the Graduate College

## ACKNOWLEDGMENTS

I'd firstly like to thank everyone from CACR who came out to Pea Patch Island with us. None of this project would have been possible without their contributions to our installation. A sincere thank you to Jack Puleo, my advisor, for his guidance through the last 2 years, and for fostering a wonderful collaborative environment in his lab. I am hugely fortunate to have been partnered to Cassie Everett on this project, whose work ethic and dedication cannot be understated. I'd like to additionally thank Delaware Sea Grant for making this research possible, Fengyan Shi and Matt Malej for their technical guidance, and DNREC for helping to facilitate our field work on the island.

Portions of this work have been concurrently published as the following (see Appendix):

Everett CL, Williams O, Ruggiero E, Larner M, Schaefer R, Malej M, Shi F, Bruck J, and Puleo JA (2022), Ship wake forcing and performance of a living shoreline segment on an estuarine shoreline. *Front. Built Environ.* 8:917945. doi: 10.3389/fbuil.2022.917945

## TABLE OF CONTENTS

LIST OF FIGURES .....	vi
ABSTRACT .....	viii

### Chapter

1	INTRODUCTION .....	1
1.1	Background.....	1
1.2	Vessel Wake Characteristics .....	3
1.3	Living Shorelines as Shoreline Protection .....	3
1.3.1	Living Shoreline Overview .....	3
1.3.2	Living Shoreline Design in Response to Vessel Wake .....	4
1.4	Wake Modelling .....	7
1.4.1	Historical Approaches .....	7
1.4.2	FUNWAVE-TVD.....	8
1.4.2.1	Model Overview .....	8
1.4.2.2	Previous Applications.....	9
2	FIELD STUDY .....	12
2.1	Intro to Site .....	12
2.2	Installation Design.....	15
2.3	Instrumentation.....	19
2.3.1	Sensors.....	19
2.3.2	Camera.....	19
2.3.3	Survey Equipment .....	20
2.3.4	Quality Control.....	20
3	MODEL SETUP AND VALIDATION .....	22
3.1	Bathymetric Grid.....	22
3.2	Vessel Course and Size .....	24
3.3	Calibration .....	26
3.3.1	Calibration of Alpha and Beta parameters .....	26
3.3.2	Final Calibration.....	27
3.3.3	Northbound Vessel .....	29
3.3.4	Southbound Vessel .....	31

3.3.5	Validation Trends .....	33
4	RESULTS.....	34
4.1	Performance of Living Shoreline Installation .....	34
4.2	Field Study Wake Data.....	35
4.3	Model Parametric Studies.....	36
4.3.1	Effect of Structure in Model.....	37
4.3.2	Vessel Speed.....	40
4.3.3	Vessel Length .....	41
4.3.4	Vessel Draft .....	43
4.3.5	Water Level .....	45
5	CONCLUSIONS AND FUTURE WORK.....	47
Appendix		
	PERMISSIONS .....	53

## LIST OF FIGURES

Figure 1. Pea Patch Island (Study Area) and the adjacent shipping channel. Figure generated by Emma Ruggiero and Mike Lerner .....	13
Figure 2. Eroded tree roots on the north shore of Pea Patch Island .....	14
Figure 3. A southbound container ship as seen from the northeast shore of Pea Patch Island. ....	15
Figure 4. Final Installation Design. Figure generated by Emma Ruggiero.....	17
Figure 5. Live stream-captured image of final installation and sensor array. ....	18
Figure 6. Diagram showing the sensor array deployed at the site.....	19
Figure 7. Model domain of bathymetry at Pea Patch Island and the adjacent shipping channel in the Delaware River.....	23
Figure 8. Close-up of installation resolved in the model grid .....	24
Figure 9. Plot of vessel paths. The yellow line shows the northbound vessel path. The red line shows the southbound vessel path. Each path extends past the edge of the bathymetry in their respective direction. ....	26
Figure 10. Effect of draft on northbound pilot study wake event. Orange line shows simulated water level, black line shows measured water level. ....	28
Figure 11. North validation data for ebb tide events .....	30
Figure 12. North validation data for flow tide events .....	30
Figure 13. Southbound validation data for ebb tide events .....	32
Figure 14. Southbound validation data for flood tide events .....	32
Figure 15. Survey data collected in May (top) and September (middle), and elevation change (bottom). Figure generated by Cassie Everett .....	35
Figure 16. Aggregated wake profile. Figure generated by Cassie Everett and Emma Ruggiero .....	36

Figure 17. Results from water level structure performance test. Left side shows relative flux without T-structure, right side shows relative flux with structure present. Shaded grey area shows area landward of head of T-structures. Dotted lines correspond to the four cross shore sensors deployed in the sensor array.....	39
Figure 18. Time series results from vessel speed test. Left panel shows northbound vessel wake simulation. Right panel shows southbound wake simulation.....	40
Figure 19. Comparison between vessel speed and maximum modelled wave height. Maximum wave height was determined using a zero down-crossing algorithm.....	41
Figure 20. Time series results from vessel length test. Left panel shows northbound vessel wake simulation. Right panel shows southbound wake simulation.....	42
Figure 21. Comparison between vessel length and maximum modelled wave height. Maximum wave height was determined using a zero down-crossing algorithm.....	43
Figure 22. Time series results from vessel draft test. Left panel shows northbound vessel wake simulation. Right panel shows southbound wake simulation.....	44
Figure 23. Comparison between vessel draft and maximum modelled wave height. Maximum wave height was determined using a zero down-crossing algorithm.....	45
Figure 24. Time series results from water level test. Left panel shows northbound vessel wake simulation. Right panel shows southbound wake simulation.....	46
Figure 25. Comparison between water level and maximum modelled wave height. Maximum wave height was determined using a zero down-crossing algorithm.....	46

## ABSTRACT

Vessel wake is a major source of wave energy in many estuaries, particularly in low-fetch areas, where energy from wind waves is limited. However, knowledge and understanding of vessel wake on the estuarine shoreline is limited. Documentation on living shoreline approaches to mitigate vessel wake is even more limited. In this study, a living shoreline design was implemented at Pea Patch Island, located on the Delaware River, to mitigate energy from vessel wake. The installation consisted of four T-shaped groins composed of coir logs, along with *Spartina patens* and *Spartina alterniflora* planted at the base of the T's. Data from this installation were used to validate the ship wake module of the nonlinear Boussinesq wave model FUNWAVE-TVD. Once validated, model simulations suggested that for more than half of the tidal range, the structure yielded 40 - 80% reduction in energy flux near the shore. With regard to ship wake generation, parametric studies indicate that velocity is the most important vessel parameter controlling maximum wave height at a given site. Vessel length and draft are also positively correlated with maximum wave height. These findings about vessel wake generation can help policy makers and engineers better understand vessel wake to mitigate the environmental consequences of wake at the shore.

# Chapter 1

## INTRODUCTION

### 1.1 Background

The past 75 years of climate change and sea level rise have demonstrated a clear threat to estuaries. Shoreline retreat is pervasive in estuaries along the east coast of the United States. From 1958 to 1998, Cedar Island, an estuarine island in North Carolina with a 58.6 km<sup>2</sup> footprint, experienced an average shoreline retreat of 0.24 m per year (Coward et al., 2010). A broader study of the Delaware estuary found a century-long average retreat rate of 1.1 m per year, with an increased rate of 2.13 m per year from 2007 to 2012 (Pijanowski, 2016). This study also directly linked modelled wind-induced wave energy with shoreline retreat rate, which suggests that shoreline retreat can be partly attributed to hydrodynamic forcing, in addition to sea level rise and the increased frequency of extreme events. The rates of shoreline retreat found in this study outpaced the rates of shoreline retreat experienced at the oceanic coasts of Southern New Jersey and Delaware. This difference is likely due to differences in the sediment composition between estuaries and coastal beaches; the finer sediment composition of many estuaries makes them vulnerable to erosion at moderate-to-high energy environments.

While wind forcing and sea level rise alone may drive shoreline retreat, wake due to recreational and commercial vessel traffic can also be a major source of wave energy, particularly in estuaries. Vessel wake has been shown to disrupt both abiotic and biotic components of estuarine ecosystems (Gabel et al., 2017). Increased

velocities observed during wake events induce higher levels of sediment suspension and thus shoreline erosion. Commercial vessels were revealed to cause much higher maximum sediment suspension when compared to smaller recreational vessels. Periods of high boating activity in the Chesapeake Bay have been linked to elevated levels of turbidity in the waterway (Bilkovic, 2019). Safak (2021) confirmed this finding, observing that ship wake in intertidal waterways increases sediment transport rate by 12%.

Shipping vessels have also increased in length and draft over time. From 1990 to 2013, the mean carrying capacity of the world's shipping container fleet increased by a factor of 6 (Tran et al., 2014). This change is driven by economic benefits of larger vessels. The "cube law" states that as a vessel's dimensions double, the carrying capacity of that vessel is cubed. While this increase in size does contribute to economies of scale, it also induces negative externalities in port costs, ground transportation costs, and channel dredging costs. There are also negative environmental consequences from the increased size and number of shipping vessels. the presence of boat traffic may increase plant biomass inhibiting maximal plant growth (Asplund et al., 1997). In Venice, researchers linked the increased prevalence of large ferries and cruise ships to the increased rate of erosion in the Malamocco Marghera Channel (Zaggia et al., 2017). GIS analysis revealed a 3 - 4 m rate of shoreline retreat per year. Over this time, the shoreline did not reach a stable profile, although the rate of retreat has slowed on average. However, yearly vessel traffic continues to rise, which leaves little reason to assume that a stable profile will be reached in the foreseeable future. Besides the environmental cost of lost ecosystems, there is a monetary cost of this erosion as well. The cost of dredging and removing

800,000 m<sup>3</sup> in this channel is 40 million Euros. Assuming that the eroded sediment is deposited into the channel, this corresponds to an average of 1.5 million Euros per year in dredging costs to maintain a navigable channel.

## **1.2 Vessel Wake Characteristics**

Vessel-generated wake generated by large commercial vessels tends to follow a distinct pattern. Low Froude number wakes tend to generate large depressions in the water surface, followed by smaller amplitude Kelvin wake (Parnell et al., 2014).

Froude number is calculated as follows:

$$Fr = \frac{V}{\sqrt{gd}} \quad (1)$$

where  $V$  is vessel speed,  $g$  is the gravitational constant, and  $d$  is channel depth.

Drawdown wake is particularly pronounced in narrow shipping channels (Ng, 2011).

This drawdown wake, also known as the primary wake, is caused by the low-pressure area that trails the vessel. Water on the shore is drawn towards the shipping channel by the pressure differential. As the pressure equalizes, a surge of water returns to the shore.

Wake amplitude is impacted by a variety of ship parameters and environmental factors. As distance from the vessel increases, wave heights decrease (Ng, 2011).

There is also a strong positive correlation between vessel velocity and wave height.

## **1.3 Living Shorelines as Shoreline Protection**

### **1.3.1 Living Shoreline Overview**

The term “living shoreline” was first used in a publication in 2008 to describe shoreline protection methods which aim to restore lost habitat, with or without

structural components (Currin et al., 2008). Traditional engineering implementations (seawalls, bulkheads) are simultaneously becoming less sustainable and cost-effective, leading to alternative approaches to shoreline protection (Smith, et. al., 2020).

Widespread adoption of hardened structures has been linked to habitat degradation (National Research Council, 2007). Properly designed living shoreline implementations have been shown to attenuate wave energy, provide a barrier to storm surge, and provide local environmental benefits (O'Donnell, 2016). These benefits include providing habitat for threatened fish and plant life, groundwater filtration, and decreased sediment transport. In comparison to traditional hardened structures, little research and design specifications exist pertaining to living shorelines. Their application may also be more dependent on local environmental factors compared to hardened structures. Widespread implementation of living shorelines thus depends on quality research demonstrating their efficacy (Morris et al., 2018).

### **1.3.2 Living Shoreline Design in Response to Vessel Wake**

While living shoreline research is far from comprehensive, research supporting the use of living shorelines in response to vessel wake specifically is even more sparse. Published design guidelines for living shorelines reflect this sparsity. In 2015, Stevens Institute published a document outlining guidelines for living shorelines (Miller et. al., 2015). This document was commissioned by the state of New Jersey and attempts to clearly outline living shoreline guidelines for engineers, regulators, and homeowners based on the best available data and information. In considering wave energy, the authors suggest increasing the weight of a shoreline protection as a function of energy based on fetch length. However, while this document refers to ship wakes as a potentially dominant energy source in sheltered waterways, it states that

“wakes are rarely if ever taken into account during design in a physically satisfying manner, due to a lack of readily available wake measurements”. Similar lapses exist in the Virginia Shoreline Management Model, which uses fetch as a catch-all for wave energy prediction, ignoring the potential impact of both recreational and commercial wake (Bilkovic et al., 2019). Many sites in areas of high recreational boat traffic on the Chesapeake Bay designated as low energy by this model are protected by hardened structures, which suggests a disconnect between the state’s guidance on shoreline protection and the needs of the community. This exclusively wind-wave-based approach demonstrates a lapse in the current body of work on living shorelines as they relate to wake. There are clear design standards to follow in this document based on fetch length and wind wave conditions but the document leaves wake design choices to the discretion of the reader, despite identifying wake as a primary energy source in certain environments. This problem could be addressed by creating general classifications of wake levels based on the prevalence of wake events, boat speed, and boat size to estimate energy levels. A potential approach to make this calculation accessible to those designing living shorelines could be to compare wake energy per hour to the equivalent wind-wave conditions that could cause similar energy levels in the water. However, one-to-one comparisons between wind-waves and wake-waves are often difficult due to the vast energy differences between the two, which has a potentially non-linear effect on erosion and the degradation of living shoreline implements.

Despite the poor documentation of ship wake energy in living shoreline design guidelines, some research has been done on living shoreline implementations in response to vessel wake. Researchers tested a living shoreline design composed of

wooden break walls and oyster gabions (Herbert et al., 2016). The design was deployed on the Tolomato River, a salt marsh estuary. In this environment, oyster reef populations have deteriorated in recent years, as evidenced by oyster rakes (dead oyster shells) and the presence of oyster reefs in nearby waterways not exposed to recreational boating. The shoreline was designed to attenuate wave energy to the point where oyster reef growth was possible, so that new oyster reefs, combined with the installed wooden structures, would protect vegetation from wave energy. A follow up study three years later found that the structure had been effective in fostering oyster reef growth and shoreline advancement (Safak et al., 2020). At all three measured sites, oyster reefs developed successfully, with percent cover of live oysters on the gabions reaching 35%, which compares to natural intertidal reefs on the same river (27.1%). Treated areas also experienced seaward shoreline advancement, while untreated areas experienced landward shoreline retreat. However, increases in vegetation density were minimal relative to untreated areas along the estuary, which suggests that more rigorous wave attenuation may be necessary to facilitate further salt marsh growth. This study provides a guide on establishing a living shoreline in a wake-dominated environment, which had been lacking in the literature. More studies like this could help to establish more general practices for installing living shorelines in estuaries defined by high energy wakes. However, this paper still leaves much to be desired in terms of wake measurement and analysis, which leaves future researchers with insufficient information to justify direct replication of the design in different environments.

## **1.4 Wake Modelling**

### **1.4.1 Historical Approaches**

Crude vessel wake models have historically been used to estimate the relative importance of vessel wake relative to tides, river flow, and wind waves. Early empirical models included a formulation for diverging wave direction based on Froude number (Weggel et al., 1986). This formulation ranged from  $35^\circ$ , the theoretical deep-water limit, to  $0^\circ$ , the theoretical value at a Froude number of one.

This formulation was based entirely on theoretical limits and experimental data describing wave direction. Transverse wave period can be determined using the assumption that wave celerity is equal to vessel speed, and the dispersion relationship (Sorensen, 1997). The final parameter that was typically modelled was the maximum wave height. This was a much more complex factor to model, given dependencies on ship speed, channel geometry, ship length, draft, and distance to the channel from a given site. As such, there were several empirical approaches to modelling maximum wave height (Bhowmik 1975, Gates et al. 1977, Bhowmik et al. 1991). Each of these formulations is based on a limited dataset. Some are only applicable for narrow channels, some for only one vessel type, and none cover the full range of velocities. Sorensen (1997) used a larger dataset from Zabawa and Ostrum (1980) to test the accuracy of three models developed with this empirical methodology. The goal was to accurately assess predictions of wake heights from an 8 m long recreational vessel. The models reasonably match the data but fail to cover a sufficient range of velocities. This limited range of velocities demonstrates an inherent problem with empirical vessel wake models. Even when controlling for vessel size and shape, distance from

shore, and channel depth, empirical models fail to cover a sufficient range of velocities accurately. There are simply too many variables for such a model to be optimal.

Wu (1987) presented a numerical alternative to modelling ship wake. The periodic and continuous pattern of ship wake generation was recreated using a generalized Boussinesq model with a moving pressure disturbance. Wu (1987) used a forced Korteweg-de Vries model due to the limited computational resources of the time. Results from this model reflected Kelvin wake patterns, as well as a moving region of depressed water level responsible for the drawdown observed from shore. The results from this model showed high levels of agreement with experimental results, especially at near-critical Froude numbers. Boussinesq models have since proven highly effective for modelling vessel wake (Torsvik et al., 2009, David et al., 2017).

## **1.4.2 FUNWAVE-TVD**

### **1.4.2.1 Model Overview**

A module for generating ship wake through a pressure term was recently incorporated in the existing fully nonlinear Boussinesq FUNWAVE-TVD model (Shi et al., 2018). FUNWAVE accommodates wave breaking by switching from dispersive Boussinesq equations to nonlinear shallow water equations at points where a breaking criterion (out of several breaking criteria possible) is reached. The model was validated using laboratory (Gourlay 2001) data based on Froude number. A viscosity-type breaker showed a higher level of agreement with lab data when compared to nonlinear shallow water equations. Ultimately, FUNWAVE-TVD is a useful tool for predicting ship wake and ship wake energy given bathymetry and vessel data.

The USACE also produced a report (Malej et al., 2019) on a sediment transport module in FUNWAVE-TVD. This module assumes quasi-steady flow, which is more appropriate for swash zone and ship-wake-induced sediment transport. It accounts for bedload and suspended sediment transport. The report also provides two examples of validation cases. One of these cases compared simulated morphology data to field data in Crescent City Harbor during a 2011 tsunami event. The model was generally able to capture the broad morphological trends but underestimated the magnitude of erosion. Poor grid resolution and an insufficient modeling period may have been the cause of this discrepancy. The other case is a laboratory experiment using sediment transport induced by a dam-break. The laboratory approach presented challenges based on the behavior of the dam-break, but the model had some agreement with the data. The USACE is involved in future work to continue validation efforts, but more validation is needed for this relatively new model, particularly for fine-grained sediment transport, which tends to have more cohesive properties. There is ample opportunity for validating both the ship wake and sediment transport modules in riverine waterways, which tend to be composed of fine-grained sediment.

#### **1.4.2.2 Previous Applications**

Since its publication in 2017, the FUNWAVE-TVD ship wake module has been used in several studies. In 2020, a study of boat wakes and their impact on salt marshes in Jamaica Bay, New York was conducted (El-Safty et al, 2020). This study was motivated by prior data and imaging suggesting that salt marshes in the area have rapidly deteriorated. Prior research has linked this deterioration to water pollutants, storm events, sea level rise, and sediment supply, but not ship wake. Jamaica Bay is highly trafficked with tugboats, high-speed motorboats, and ferries of varying size,

which motivated research to determine what role, if any, ship wake has played in the decline of salt marshes. Direct field-to-model comparison was not possible in this study due to insufficient vessel information for each given wake event. Instead, a typical vessel and path were used to generate a wake signal. Using the sediment transport module in FUNWAVE-TVD yielded a few major assessments of shoreline impact of ship wakes. For one, ship wakes tended to generate erosion along shipping channels, particularly at the edge of marshy areas. Additionally, there was a nonlinear relationship between erosion and number of vessels. As the number of vessels increases, the cumulative erosion increases by an even greater factor. This nonlinear relationship has significant implications for design considerations based on ship wake recurrence. Finally, the researchers concluded that slow moving vessels caused negligible erosion, while higher vessel speeds (greater than 7 m/s) resulted in cumulative bed elevation changes, particularly in shallow areas along shipping channels. As with the prior report from the USACE, this study has inherent uncertainty based on the behavior of cohesive sediment. Morphological data could not be verified because of the insufficient shoreline data from Jamaica Bay. This study is a great example of the useful application of FUNWAVE-TVD, but also the limited extent to which field data have been validated using exact vessel parameters.

A study published in 2020 compared FUNWAVE-TVD ship module outputs to field measurements collected along the Tolomato River. The field data from this study highlight the difficulty of working with ship wake. Different vessel types produce distinctly different wave patterns, as evidenced by the diversity of spectrogram shapes. This study used Froude number to categorize wake events. Some wake events were connected to vessels tracked by the U.S. Coast Guard Automatic Identification System

(AIS), but most small vessels are not tracked by the AIS, so only a minority of the recorded wake events had corresponding AIS data. Even further, because of the wake climate in the river, researchers could not directly link any single wake event to a corresponding AIS data set. However, comparisons between an analytical model and numerical model (FUNWAVE-TVD) outputs did yield more fruitful results. This analytical model was based on a Gaussian vessel shape whereby the draft is dependent on the length and width of the vessel. Simulations of this type were performed in a flat domain bounded by sponge layers. The data comparison suggested that FUNWAVE-TVD drawdown wake simulation results were within 5% error of the analytical model for low Froude number wakes (large container ships, for example), but displayed lower levels of accuracy for wakes from faster-moving vessels, particularly when generated from the deepest parts of the channel, as shallow water assumptions are not as valid for these wakes as those from slow moving ships. Despite this area of inaccuracy in wake generation, the model still performed well compared to an analytical solution for all cases in predicting the shallow water evolution of wake waves, which is essential for modeling sediment transport processes and the behavior of wetlands. This study further proves the utility of FUNWAVE-TVD as a tool for accurately modeling ship wakes, and also demonstrates a clear need for field validation using real ship data.

## **Chapter 2**

### **FIELD STUDY**

#### **2.1 Intro to Site**

Pea Patch Island is a river silt deposit formed island located in the Delaware River (Figure 1). The study area is located on the north side of the island, directly adjacent to the shipping channel. Pea Patch Island functions as one of the largest nesting areas of wading-birds on the entire east coast (Parsons, 1995). The island is also home to Fort Delaware, a historic military fort and tourist attraction. The fort and the island itself are both listed on the National Register of Historic Places. The northeast side of the island has experienced high levels of erosion for decades (Figure 2) (Brady, 1997). The US Army Corps of Engineers (USACE) constructed a small seawall on the south-east corner of the island to protect the historic fort on the south side of the island. The north side of the island is now particularly prone to erosion because it is not protected by the seawall and lies a mere 500 - 1000 m from the dredged shipping channel that extends to Wilmington and Philadelphia (Figure 3). The northeast corner, home to the fort and closest to the shipping channel, has hardened protection to protect from ship wake forcing. The rest of the north face of the island lies unprotected from ship wake. This area is home to a forest which is vital to the island's function as a heronry, but whose existence is threatened by the continual erosion of the shoreline due to wake.

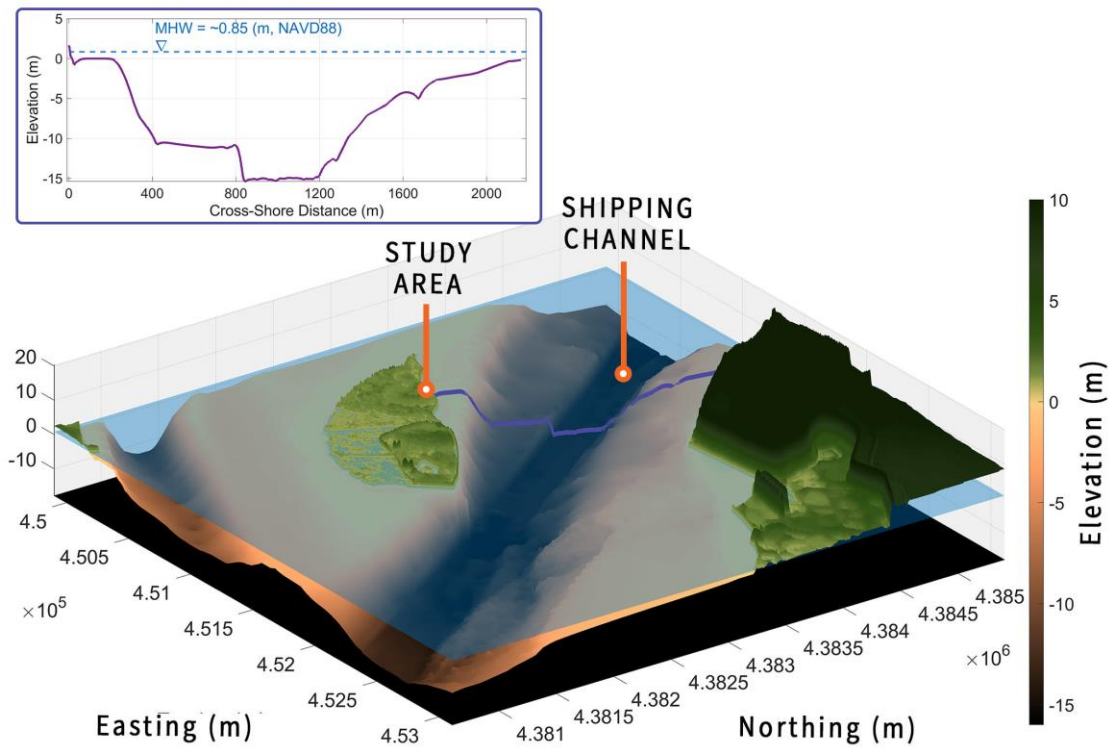


Figure 1. Pea Patch Island (Study Area) and the adjacent shipping channel. Figure generated by Emma Ruggiero and Mike Larner



Figure 2. Eroded tree roots on the north shore of Pea Patch Island

Large vessel traffic in the Delaware river accounts for ~20% of the country's crude oil imports (CAIT, 2012). There are also several petroleum refineries along the shoreline, which combined, process nearly a million barrels of crude oil per day. As such, it is an essential and busy hub for commercial vessel travel. To allow for larger vessels, the channel was deepened to 13.7 m and widened at bends in 2020. Vessel traffic and size have increased over time, an increase which is projected to continue until at least 2050. These increases, combined with expected sea level rise, pose a potential threat to silty estuaries like Pea Patch Island.



Figure 3. A southbound container ship as seen from the northeast shore of Pea Patch Island.

## 2.2 Installation Design

Prior living shoreline designs in the mid-Atlantic have featured the use of coir logs, wood bundles, and oyster bags. Coir logs are used as temporary but biodegradable shoreline protection which allows vegetation to establish strong root systems (O'Donnell 2016). In low energy environments, coir logs can last three to five years, but almost no research has been done on coir logs in medium-to-high energy environments. As such, two pilot tests were performed to test the feasibility of these materials at the site. The first pilot test involved coir matting wrapped around bagged oyster shells, as well as traditional coir logs. This design intended to add density to the

buoyant coir matting, while also yielding the ecological services associated with oyster reefs (Smyth et al., 2015). While this design was highly resilient, the weight of the coir-wrapped oyster bags would be an obstacle to the constructability of a full-scale installation. The second pilot study featured a T-shaped groin, based on a design used in Vietnam (Albers, 2018). The design in Vietnam was aimed at limiting wave height and runup during storm events in locations with little to no mangrove protection. The T design was appealing because it performed excellently at high energy levels in Vietnam. The length of the groin was composed of coir logs, this time staked down to prevent the logs from mobilizing, while the head of the groin was composed of a brush bundle composed of local driftwood. The structure failed due to buoyancy issues. The sisal twine used to secure the brush bundle failed due to friction from the wood, and the jetted wooden piles used to secure the coir logs did not generate enough friction to prevent coir logs from floating away.

The pilot study demonstrated that the coir logs themselves could be a resilient material if they were prevented from mobilizing. To solve the buoyancy issue, a motorized post driver was used to drive 3 m piles to secure the coir logs. Because this method avoided jetting the posts into place, which would have created a hole larger than the width of the pile, the piles experienced more friction and remained in place.

The final design was composed of four T-structures aligned landward (Figure 4). The bases of the T's were 18 m long, and the heads were 9 m long. Each coir log is 3 m long. The two most landward coir logs on each T were 0.4 m in diameter, while the rest were 0.5 m. The coir logs used for the heads of the T's were wrapped in additional coir matting, which was secured by sisal twine. The heads of the structures were separated by 6 m. The separation was decided by scaling-down the design of the

T-structure from the Vietnam study (Albers, 2018). The structure was constructed by a team of 15 volunteers and researchers over the course of 2 days in June 2021. Each coir log was secured with 5 sets of sisal twine tied to wooden piles across the log. After the sisal twine was tied to the drilled piles, the piles were drilled one additional time to ensure that the sisal twine was in tension. This measure was intended to restrict the mobility of the coir log to avoid frictional failure in the sisal twine and coir matting. *Spartina alterniflora* and *Spartina patens* were planted densely at the base of the T's, with the expectation that the protected environment would allow these plants to take root and establish a marsh.

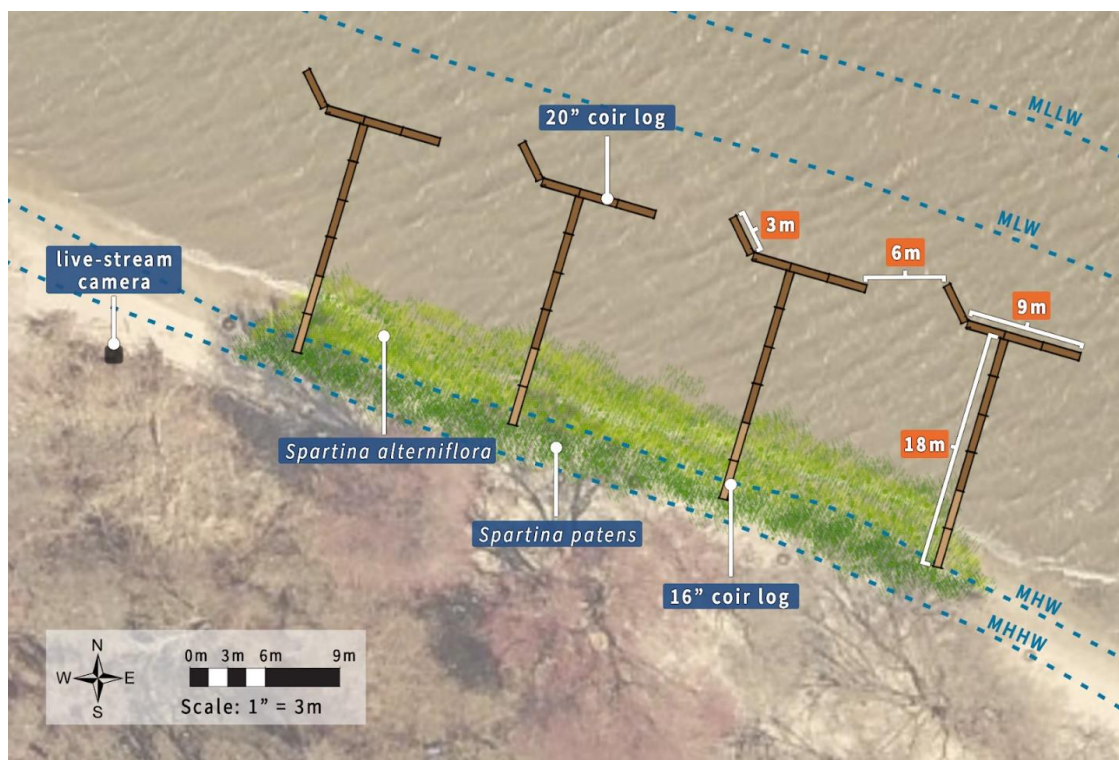


Figure 4. Final Installation Design. Figure generated by Emma Ruggiero.



Figure 5. Live stream-captured image of final installation and sensor array.

FUNWAVE-TVD was used for preliminary testing of the design. These simulations of different vessels sizes, speeds, and heading estimated maximum velocity and wave height with and without the structure present. The structure displayed a maximum blocking efficiency of 70% for velocity and 40% for wave height. The structure also performed better for northbound wakes, as anecdotally, these events had a much larger drawdown and longshore current seen from the site. There were high velocities in the nearfield of the structures, indicating some potential for local scour near the structure. However, the modeled version of the structure was significantly less porous than the actual coir logs deployed at the site, which would allow water to flow through the structure rather than around it.

## 2.3 Instrumentation

### 2.3.1 Sensors

A grid of sensors was deployed to measure the cross-shore and along-shore propagation of boat wake (Figure 6). The along-shore transect consisted of sensor locations A1-A5, while the cross-shore transect consisted of sensor locations C1-C4. Note that the A3 and C1 locations are the same but named separately in each transect. At each grid location shown, RBR compact pressure gauges and JFE velocity sensors were deployed. The RBR sensors were deployed 0.01 m above the bed, and JFE sensors were deployed 0.1 m above the bed, facing seaward. Two additional RBR sensors were used onshore to detect atmospheric pressure.

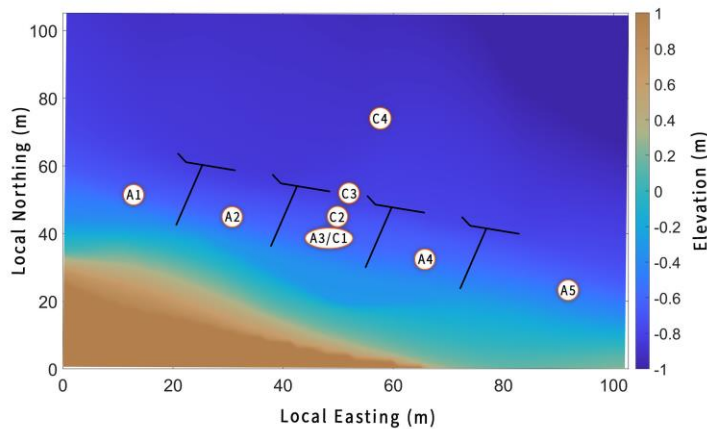


Figure 6. Diagram showing the sensor array deployed at the site.

### 2.3.2 Camera

Two cameras were placed at the site to identify wake events. The first was a

Brinno TLC200 time lapse camera, set to record an image once every 10 s. This camera was deployed for 2-week long intervals, since it is battery powered. The second camera used was a 1080p livestream camera with 3x zoom powered by solar panel from Erdman Video Systems, Inc. Footage from this camera could only be accessed at 1 frame per minute. While the Brinno provided footage of wake events with higher temporal resolution, the Erdman camera captured footage for the entire duration of the installation. Together, these cameras provided a comprehensive understanding of site conditions at the installation.

The footage from these cameras was used to generate a log of wake events recorded between July 1<sup>st</sup> and August 18<sup>th</sup>. The video was used to determine the time of each vessel passage, the type of vessel (tug, barge, speedboat), and the direction of travel.

### **2.3.3 Survey Equipment**

In May and September of 2021, elevation surveys were collected using a Leica Global Navigation Satellite System (GNSS) real-time kinetic global positioning system (RTK GPS), referenced to UTM zone 18 and NAVD88. Surveys were used to update the bathymetric grid and to evaluate the performance of the living shoreline installation.

### **2.3.4 Quality Control**

Pressure sensor data were adjusted for atmospheric pressure, and subsequently converted to depth using the hydrostatic pressure expression

$$d = \frac{P}{\rho g} \quad (2)$$

where  $P$  is pressure and  $\rho$  is typical density of brackish water  $1013 \text{ kg/m}^3$ . The next step taken to process the pressure sensor data was to filter out the tide using a moving mean filter with a window length of 312.5 s (5000 points for a 16 Hz sensor). This moving mean was subtracted from the original signal. Using the time log generated from camera footage, wake events were matched to their corresponding time series. The drawdown amplitudes were sufficiently high that within a 40-minute window from the time in the log, the minimum recorded water level was always the point of maximum drawdown. This instance was used to align the time series around the maximum drawdown. In model runs, this maximum drawdown typically occurs at a time of 300 - 400 s. As such, wake time series were translated such that their minima occurred at  $\sim 400$ s.

## Chapter 3

### MODEL SETUP AND VALIDATION

#### 3.1 Bathymetric Grid

The original bathymetric data for this study were collected in a survey following Hurricane Sandy in 2012. The local bathymetry was altered to better reflect recent survey data collected in 2018, 2020, and 2021 (Figure 7). These data include low tide surveys using GPS and channel bathymetry from the USACE. The data were spliced with the existing bathymetry using inverse distance weighting interpolation. Despite this work, minor inconsistencies remained in surveyed areas, and non-surveyed areas likely contained further inconsistencies. Bathymetry was converted to model domain by subtracting the easting and northing coordinates of the southwest corner of the grid from the easting and northing coordinates. The grid is 2399 x 2799, with x-spacing of 1.34 m and y-spacing of 1.72 m.

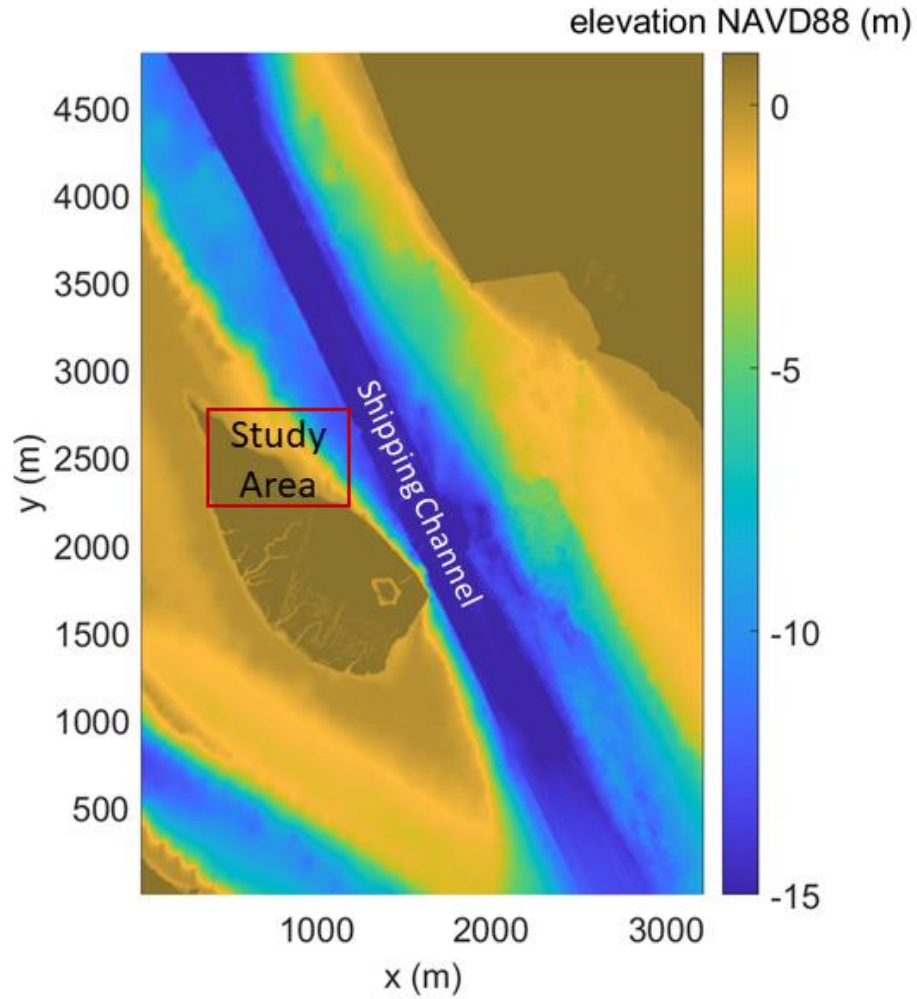


Figure 7. Model domain of bathymetry at Pea Patch Island and the adjacent shipping channel in the Delaware River.

To add the T-structures into the bathymetry, the coordinates of each log were recorded using a Leica GPS sensor, and the closest grid point to each surveyed

location was raised by 0.4 m or 0.5 m depending on the size of coir log present. The coarseness of the grid and angle of the shoreline caused the shape of the T's to warp slightly in the bathymetry (Figure 8).

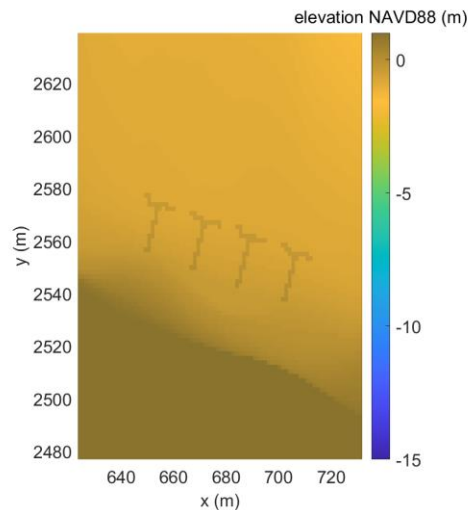


Figure 8. Close-up of installation resolved in the model grid

### 3.2 Vessel Course and Size

AIS data were used to identify ship information based on the time of a wake event. This dataset included vessel telemetry information with a timestep of 10 s, as well as vessel size information. To extract only large vessel events, the list of vessels was restricted to the following: length greater than 100 m, maximum draft greater than 5 m, and width greater than 15 m. Vessels with a velocity of zero were also filtered out to remove stationary oil tankers in nearby Delaware City. Wake events from the camera-generated log were matched with specific vessels by matching the time of the wake event to a corresponding entry in the AIS data. This methodology introduces a few problem cases. The first case which had to be eliminated from the dataset was two

ships passing the island within 20 minutes of one another. Vessels passing the island within 20 minutes of one another were sometimes misidentified using this algorithm, and so successive events were removed from the dataset.

The telemetry information from the AIS data was converted from geographic coordinates into local easting and northing, where the southwest corner of the bathymetry corresponds to the point (0,0). The first recorded point, typically outside the bathymetry, is set to time 0. The vessel course is then interpolated to a 15 s timestep. After the last point in the AIS dataset, the last two points are used to extrapolate the vessel's final velocity. The vessel is then set to run out of the bathymetry until 1800 s. The vessel courses are relatively smooth using a time step of 15 seconds (Figure 9). If this were not the case, cubic spline interpolation would have been used to smooth the vessel path, given that large commercial vessels tend not to make sharp turns.

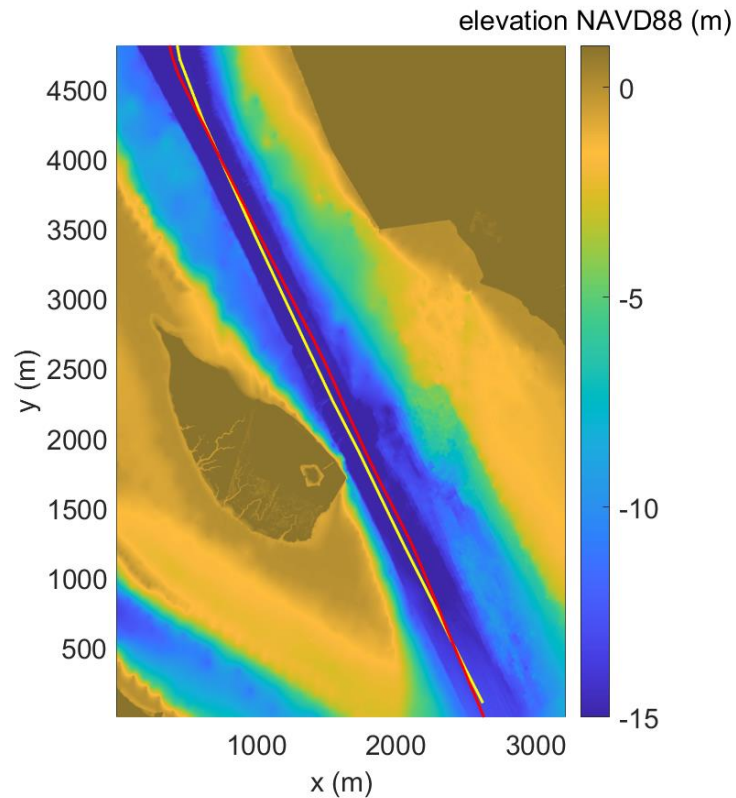


Figure 9. Plot of vessel paths. The yellow line shows the northbound vessel path. The red line shows the southbound vessel path. Each path extends past the edge of the bathymetry in their respective direction.

### 3.3 Calibration

#### 3.3.1 Calibration of Alpha and Beta parameters

Model calibration took place over two stages. The first stage involved calibrating for shape parameters using data from pilot study 2. These three shape parameters,  $\alpha_1$ ,  $\alpha_2$ , and  $\beta$ , determine the geometry of the front, back, and sides of the vessel respectively. These parameters range from 0 to 1, with 0 representing a more rounded bottom, and 1 representing a flat, square bottomed vessel.  $\alpha_1$ ,  $\alpha_2$ , and  $\beta$  were calibrated under the assumption that they would be close to uniform for most

commercial vessel shapes. The set of parameters that best matched the pilot study data were  $\alpha_1$ ,  $\alpha_2$ , and  $\beta$  equal to 0.2, 0.2, and 0.8 respectively. The low  $\alpha_1$  and  $\alpha_2$  values indicate a rounded front and back of the vessel. The relatively higher  $\beta$  values indicate a more rectangular side profile of the vessel. Once the final installation data were collected, these shape parameters were applied, and wake events were then calibrated by adjusting draft to best fit. Calibration was done based on data from sensor C4, the most offshore sensor on the cross-shore transect. This sensor is the farthest from the structure, and thus contains a wake signal that is relatively unaltered by breaking, shoaling, and reflection associated with the structure.

### **3.3.2 Final Calibration**

Given that shape parameters were held constant for all model runs, and other geometric parameters were fixed based on AIS data, the model was calibrated using draft, the only unknown quantity. Draft is reported in AIS data as maximum draft, but vessel draft varies widely based on the extent to which the vessel is loaded. The range of vessel drafts also causes large variability in the modeled wake profile (Figure 10). Increasing the draft by even a meter has noticeable effects on wake amplitude. This variability, combined with the strong effect of draft in the model, made draft an apt candidate to optimize for validation.

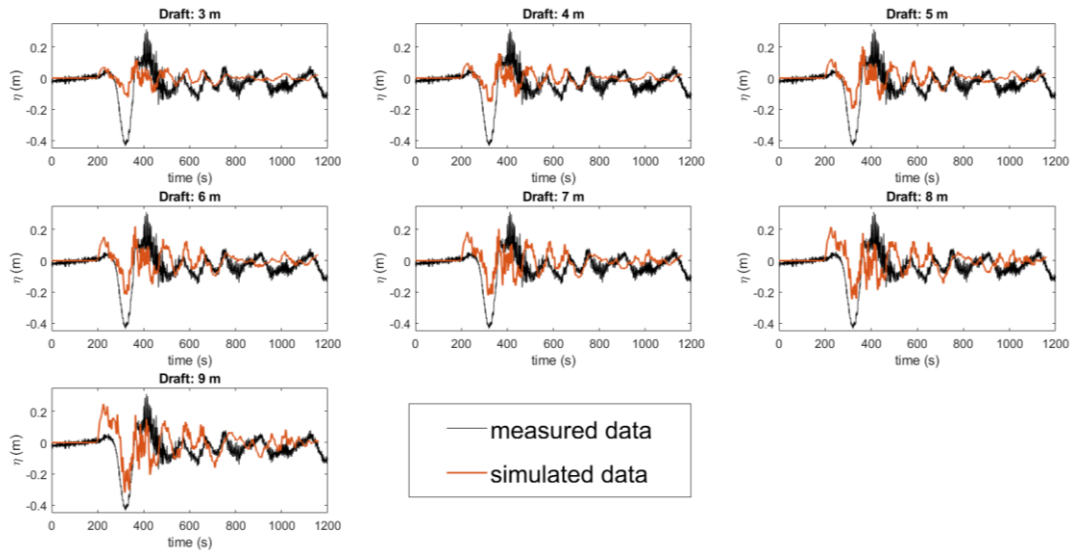


Figure 10. Effect of draft on northbound pilot study wake event. Orange line shows simulated water level, black line shows measured water level.

Calibration of draft was performed on 20 total wake events, split into 10 northbound and 10 southbound vessels because of the stark contrast between the wake patterns on shore depending on the vessel direction. The contrast may be due to the oblique orientation of the shoreline relative to the shipping channel, causing southbound Kelvin wakes to propagate normal to the shore. As such, southbound wake events tend to have higher amplitude Kelvin wake when compared to northbound events. Because the Delaware River is tidal, these 10 simulations were split into flood and ebb tides to determine if FUNWAVE-TVD's inability to model current affected wake validation in tidal environments. Validation was performed initially from a qualitative standpoint, but as results became more final, numerical comparisons of error were used to determine best fit. These comparisons include percent error in drawdown and seiche amplitude. The drawdown amplitude is

measured as the difference in maximum elevation of the small surge prior to the drawdown, and the minimum surface level reached at peak drawdown. The seiche wake amplitude was measured as the first low amplitude wave height following the much higher amplitude Kelvin wake. The amplitude of Kelvin wake itself was not used for validation, as model results tended to vastly overpredict or underpredict Kelvin wake, which was not responsive to draft adjustments. A simulation that overpredicted Kelvin wake, based on vessel path, length, and width, tended to overpredict Kelvin wake regardless of draft.

Because of inconsistencies between the modeled and real bathymetry, there was little agreement in the phasing between real and modeled runs, even when times were matched exactly (based on vessel path). As such, model runs and real data were aligned using the point of maximum drawdown. This alignment assisted in visually assessing the likeness between model simulation and reality. However, due to these phasing issues, model fit is primarily measured based on wave amplitude alone.

### **3.3.3 Northbound Vessel**

Northbound validation was mostly successful. Eight of the ten modelled events simulated drawdown amplitude within 15% error. Errors in Figure 11D were due to overprediction of seiche amplitude combined with underprediction of drawdown. Both have a positive relationship with draft, so these errors cannot be reconciled simultaneously. Figure 12D illustrates a similar problem. These two events may suggest that adjustments are needed in the  $\alpha$  and  $\beta$  parameters going forward.

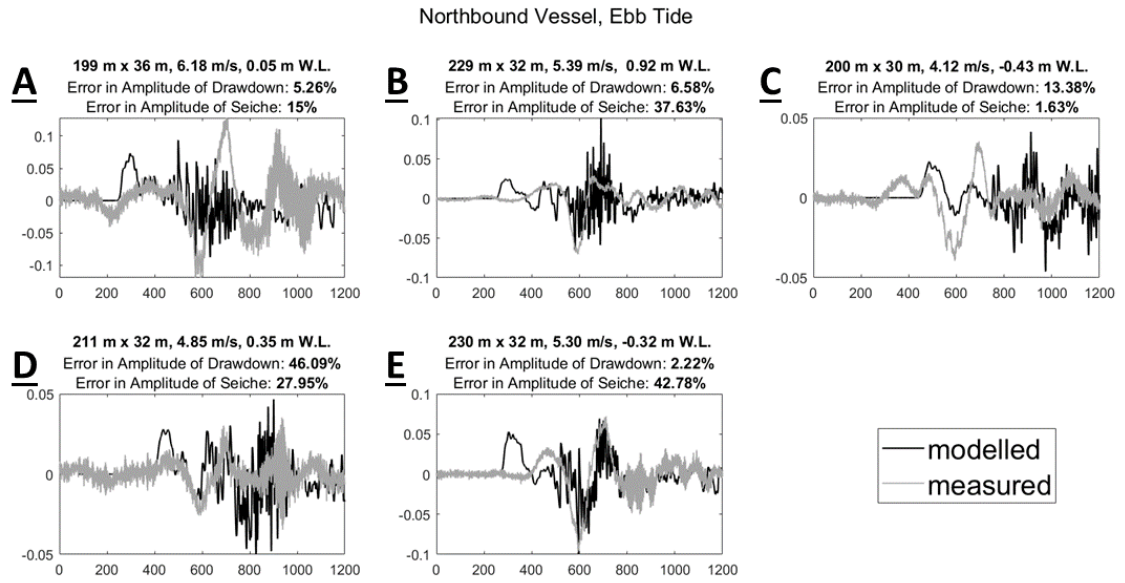


Figure 11. North validation data for ebb tide events

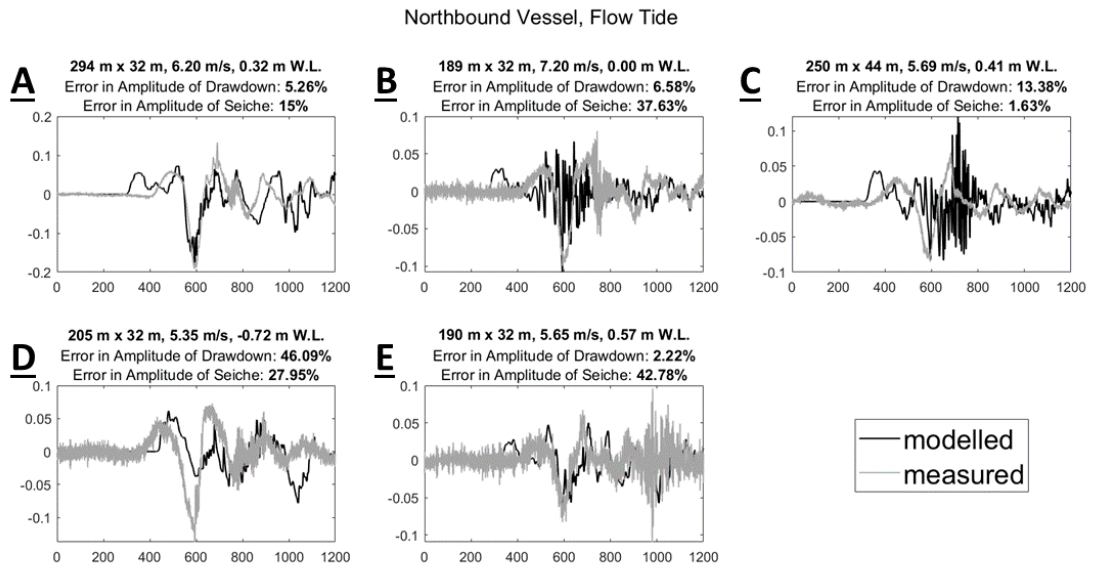


Figure 12. North validation data for flow tide events

### 3.3.4 Southbound Vessel

Southbound vessel wake validation, by comparison, was less successful. Only two wake events were modelled within 15% error in drawdown amplitude (Figures 13C, 14E). Poorly validated events demonstrated a similar, but more pronounced problem as in the two poorly validated northbound wakes. For example, in Figure 13E drawdown is underpredicted with 58.9% error, but seiche amplitude is overpredicted with 22.47% error. Once again, by merely adjusting draft, there is no way to minimize these errors without impacting the other. Many of these wake events also do not fit the typical large vessel wake profile defined by a high amplitude primary depression wake (Figure 16). For example, Figure 14C displays an event with a Kelvin wake amplitude approximately four times larger than the drawdown amplitude, which is atypical for large container vessel wake events. Because the three shape parameters were validated with a typical wake profile, they may not be suited for a wake of this type. Another specific problematic case is the one shown in Figure 13D. The model overpredicts the drawdown with an error of 109.45%, with a draft of 4.5 m. For a vessel of this size, a draft less than 4 m would be unrealistic (Clarksons, 2011), so there is no way to generate better agreement solely tuning these parameters.

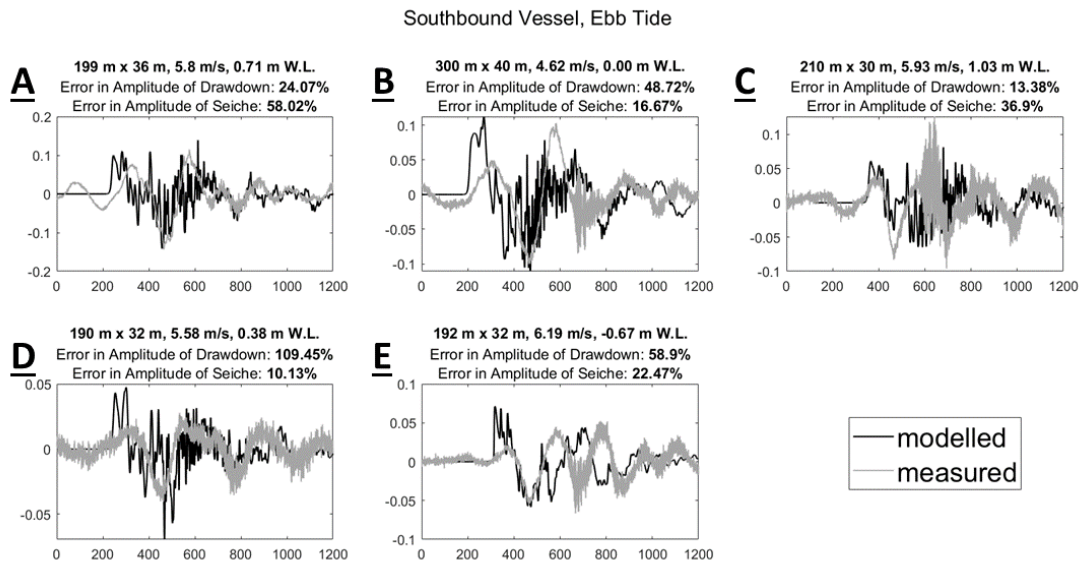


Figure 13. Southbound validation data for ebb tide events

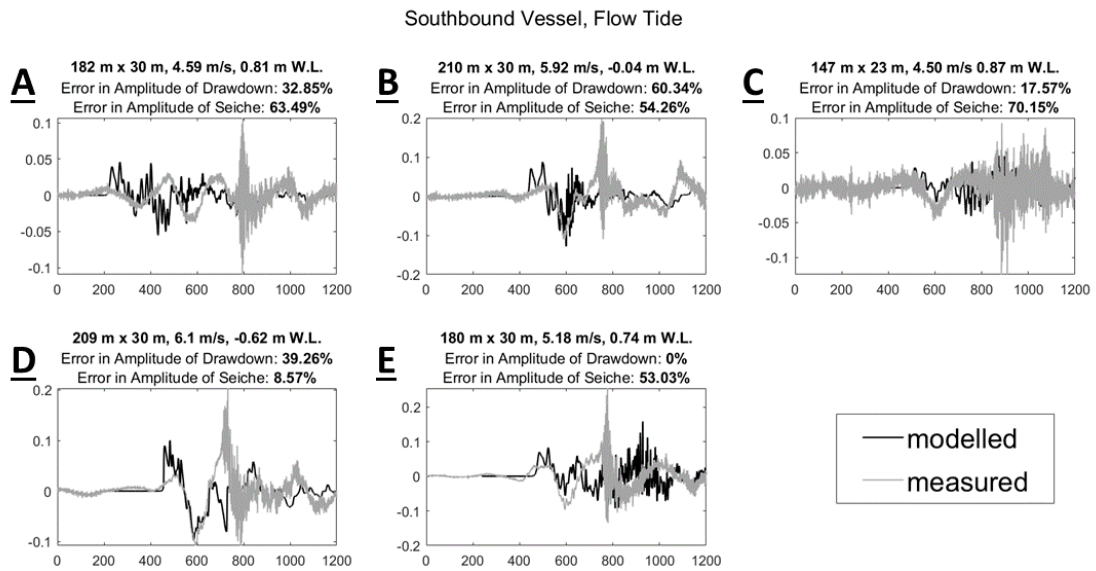


Figure 14. Southbound validation data for flood tide events

### **3.3.5 Validation Trends**

Water level, vessel length, and vessel speed had virtually no correlation with model error. However, the average error in drawdown amplitude for northbound wakes was 15.2%, while the average for southbound wakes was 40.5%. This contrast is less stark for seiche amplitude, but northbound wake events still show better agreement with field data. This may be because initial calibration of shape parameters was conducted using northbound data. The difference between average error for ebb and flow tides was negligible. However, the missing effect of current was not necessarily negligible in the model. It is possible that the error from missing tidal flow affects ebb and flood tides equally.

## Chapter 4

### RESULTS

#### 4.1 Performance of Living Shoreline Installation

Improvements in design based on the two pilot studies successfully secured the wooden piles in the sediment. However, storm surge conditions degraded the quality of the structure. After repeated storm events, much of the sisal twine failed, likely due to excessive friction, which allowed several coir logs to be displaced northward along the shore. Although maintenance was performed, the saturated coir logs were too heavy to be moved back into their original position in the structure given the resources available at the time, and additional coir logs continued to mobilize via sisal twine failure. With a more robust material used to secure the coir logs, the installation may have fared better in storm surge conditions. The majority of planted *Spartina alterniflora* and *Spartina patens* were uprooted. The island is a nesting ground for herons and is trafficked by geese and other large birds as well. As such, it is likely that these birds fed on the plants at low tide. Measures designed to discourage birds from feeding on the plants may have improved the survival rate of the plants.

Surveys before and after the installation (Figure 15) show small amounts of accretion and erosion over the four months. Areas of accretion included the midpoints of the Ts in the cross-shore direction, as well as the landward end of the three southmost T's. These areas experienced average elevation increases of ~0.1 m. There was also mild accretion seaward of the head of the T structures. Areas of erosion included the landward side of the head of the structures, as well as the landward tip of the northmost structure. The erosion at the northmost structure was the most pronounced change measured at -0.3 m. Erosion at this specific structure is likely due

to longshore current effects during wake events. The erosion landward of the head of the T's was likely due to local scour caused by the channeling of wake drawdown through the head of the T's, which was observed anecdotally on site. However, these results may be partially explained by seasonality. A multi-year set of monthly surveys may be needed to draw more salient conclusions about the effect of the structure on sediment transport.

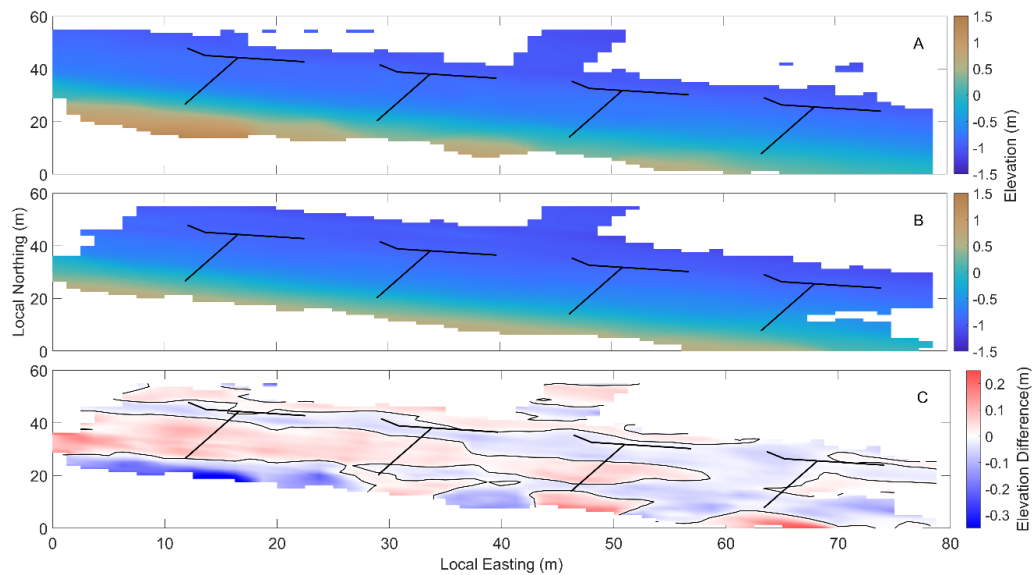


Figure 15. Survey data collected in May (top) and September (middle), and elevation change (bottom). Figure generated by Cassie Everett

## 4.2 Field Study Wake Data

1118 wake events were recorded between July 1<sup>st</sup> and August 12<sup>th</sup>, yielding an average of 26 wake events per day. The general wake profile for these events matched expectations for large commercial vessels based on the literature (Figure 16). The start

of a wake event was characterized by a slight water level increase, followed by a sharp drawdown. This drawdown was followed by a subsequent surge similar in magnitude. The water level then fluctuates at a lower amplitude as a result of seiching in the channel. Approximately 20 minutes after the initial increase in water level, the seiching dampens with a return to background conditions.

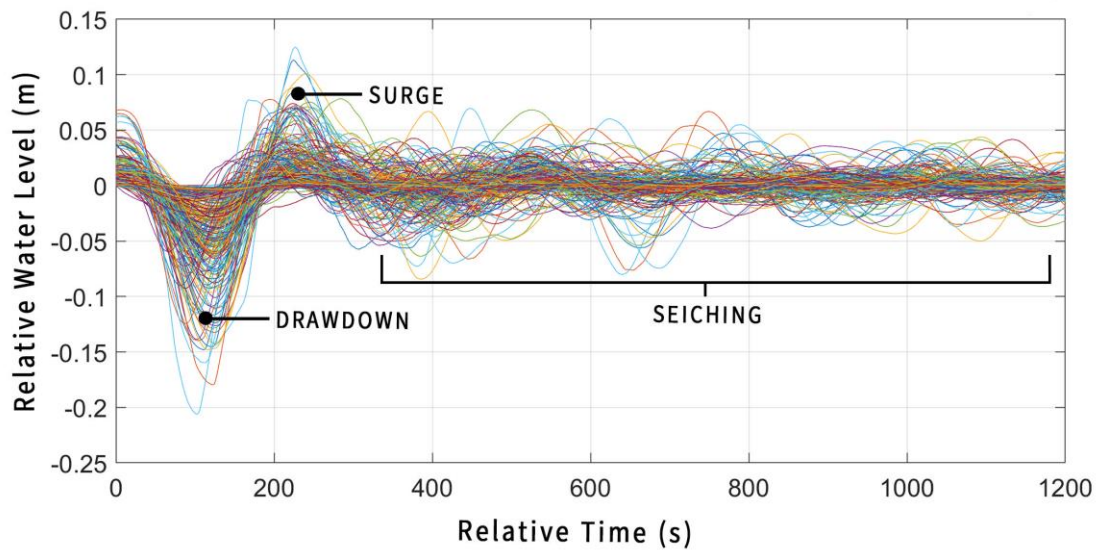


Figure 16. Aggregated wake profile. Figure generated by Cassie Everett and Emma Ruggiero

### 4.3 Model Parametric Studies

The best validated vessel wake events, one northbound and one southbound, were used to test the impact of vessel speed, water level, and vessel size on wake environment. The northbound vessel used for parametric studies was the MSC RONIT R, which has a length of 294 m, width of 32 m, draft of 9.5 m, and an average velocity of 6.20 m/s (Figure 12A) The southbound vessel used for parametric studies was the

ELANDRA FALCON, which has a length of 277 m, width of 32 m, draft of 9.0 m, and an average velocity of 5.8 m/s (Figure 13A). Maximum wave height, which is typically the drawdown amplitude, was used to evaluate the wake environment in response to changing model parameters. Maximum wave height was determined using a zero down-crossing routine in MATLAB.

#### 4.3.1 Effect of Structure in Model

Model simulations were performed at six water levels (-0.25, 0.00, 0.25, 0.50, 0.75, 1.00 m NAVD88) with and without the T-structures in the bathymetry to evaluate the effectiveness of the structures. These water levels represent the tidal range in which the most landward pressure sensor would be wetted for the entire wake event. A relative energy flux, normalized by the flux at sensor C4, was used to compare the different wake environments depending on water level. Relative energy flux was measured along a 50 m cross shore transect starting from sensor C1. Depth integrated energy flux is calculated at each timestep according to the general definition

$$E_k = 0.5\rho(u^2 + v^2) \quad (3)$$

$$F_x = E_k(h + \eta)u + (h + \eta)ug\eta \quad (4)$$

$$F_y = E_k(h + \eta)v + (h + \eta)vg\eta, \quad (5)$$

where  $v$  is the alongshore component of velocity,  $u$  is cross-shore component of velocity,  $E_k$  is kinetic energy,  $h$  is the still water depth at the sensor,  $\eta$  is water surface displacement, and  $F_x$  and  $F_y$  represent integrated energy flux in the  $x$  and  $y$  directions.

At water levels above 0.50 m, the effect of the structure appears to be negligible. Energy flux tends to evolve nearly identically in cases with and without the structure. However, at lower water levels, the effect of the structure is clear. In the northbound vessel case, all three tests below 0.50 m have greatly reduced energy

fluxes because of the structure. The decrease in energy flux is more pronounced as water level decreases. There is some reflection causing relative energy fluxes above greater than 1 just offshore of the head of the structure, but it is only responsible for less than a 5% increase in flux. The southbound case indicates similar performance to the northbound case landward of the structure but shows high levels of reflection for the -0.25 m simulation. This reflection is responsible for a 20% increase in wave energy flux. This enhanced reflection may be due to the more shore-normal direction of southbound wake, which would reflect more directly off the head of the structure. Similar reflection may be present for northbound waves, but since northbound wake waves are less normally incident, they would not propagate directly back through the center of the structure.

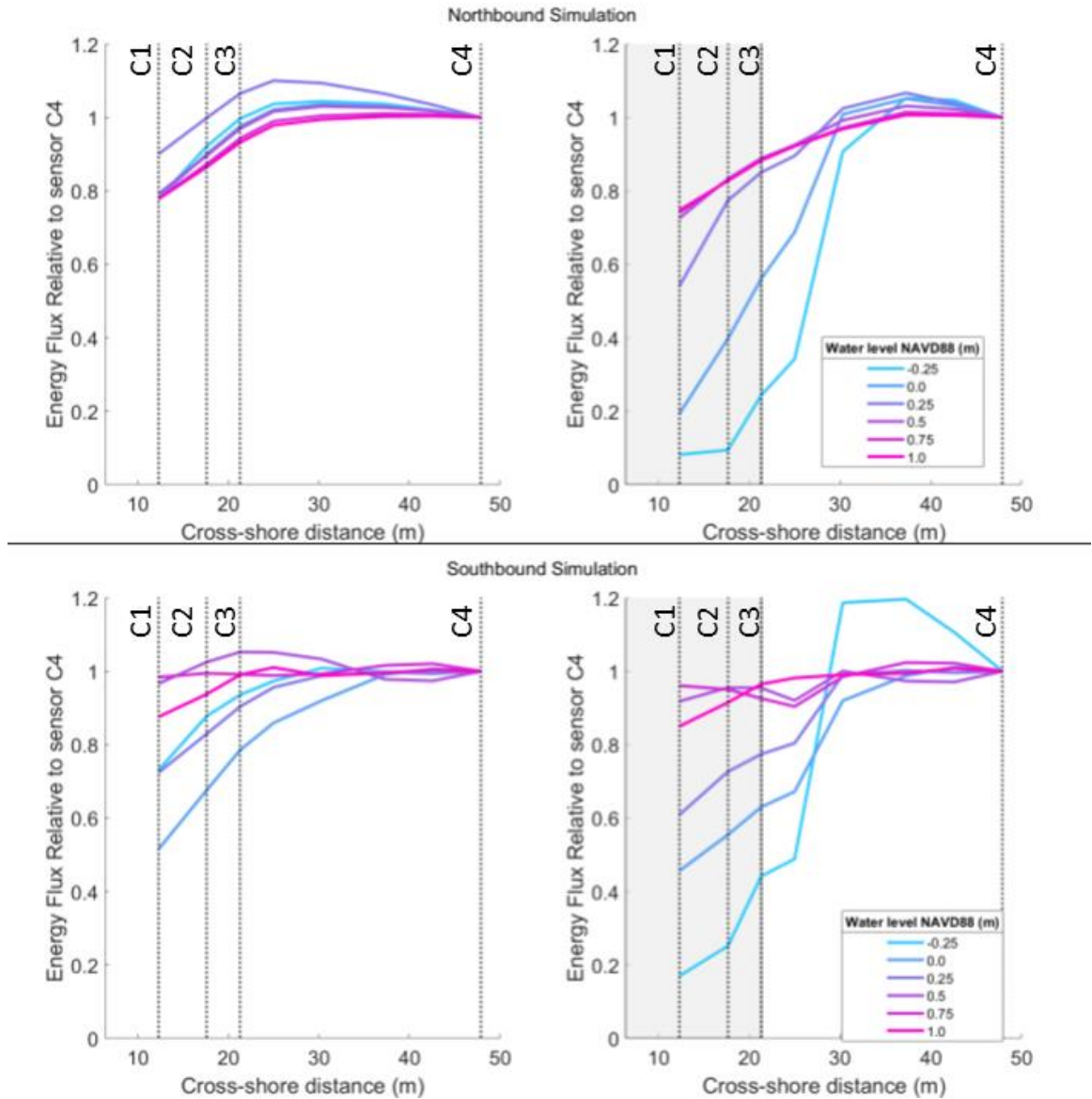


Figure 17. Results from water level structure performance test. Left side shows relative flux without T-structure, right side shows relative flux with structure present. Shaded grey area shows area landward of head of T-structures. Dotted lines correspond to the four cross shore sensors deployed in the sensor array.

### 4.3.2 Vessel Speed

Vessel speed has been shown to have a strong positive relationship with wave height. The 20 wake events used for validation had an average velocity range of 4.19 to 7.20 m/s. As such, the two wake events were simulated using velocities ranging from 3 - 8 m/s (Figure 18). This range provides a comprehensive understanding of the wake conditions associated with typical vessel travel. The 3 m/s and 8 m/s simulations, while out of the range observed in the study, provide insights into the impact of potential changes to the shipping environment., like a dredged channel allowing faster vessel travel, or legislation limiting vessel speeds in estuaries.

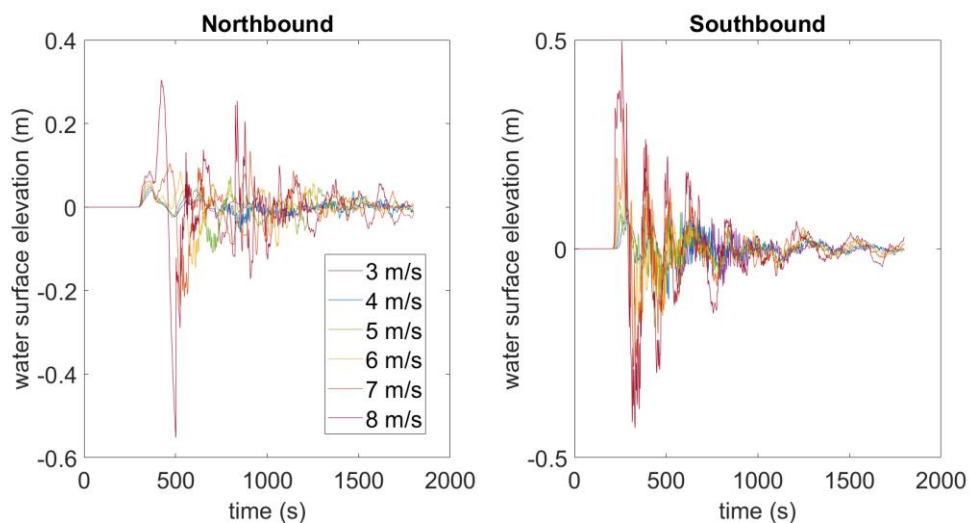


Figure 18. Time series results from vessel speed test. Left panel shows northbound vessel wake simulation. Right panel shows southbound wake simulation.

The results of this study were unambiguous. Higher velocities are strongly correlated with higher drawdown and seiche wake. This conclusion is commensurate with established theory that drawdowns are caused by negative pressure associated

with drag along the ship length. According to Bernoulli's principle, pressure is proportional to the square of velocity, so this relationship becomes increasingly apparent as velocity increases. Over the validated parameter space between 4 and 7 m/s, the maximum wave height approximately quadruples (Figure 19), which is the single largest difference in wave height over the parameter space of any variable tested.

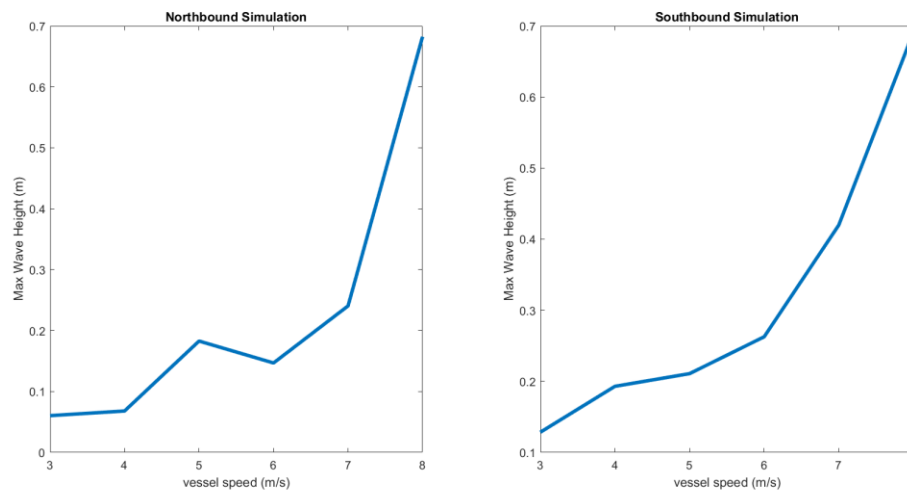


Figure 19. Comparison between vessel speed and maximum modelled wave height. Maximum wave height was determined using a zero down-crossing algorithm.

### 4.3.3 Vessel Length

A study of recreational boat wakes found a strong correlation between wake energy and vessel length cubed (Shuster et al., 2020). Such a strong connection warrants investigation into the relationship between wake energy and vessel length for larger commercial vessels. The lengths observed in the validated cases ranged from

149 m to 300 m. As such, the first length values tested were 150, 200, 250, and 300 m. These values cover the range from panamax shipping vessels to much smaller oil tankers and container ships. For the range of lengths initially tested, the relationship between vessel length and maximum wave height was much weaker than the relationship between velocity and maximum wave height. As such, the range of modelled ship lengths was expanded to include a 400 m vessel to determine if expanding the parameter space yielded a different effect on wave height (Figure 20). The 400 m vessel followed a similar trend. Increased vessel length did not have nearly the impact on wave amplitude compared to increased velocity. It is also worth noting that in the Southbound wake profile, the Kelvin wake increased disproportionately relative to the seiche and drawdown amplitudes. Despite a weaker relationship than with velocity, maximum wave height still approximately doubled over the parameter space tested (Figure 21).

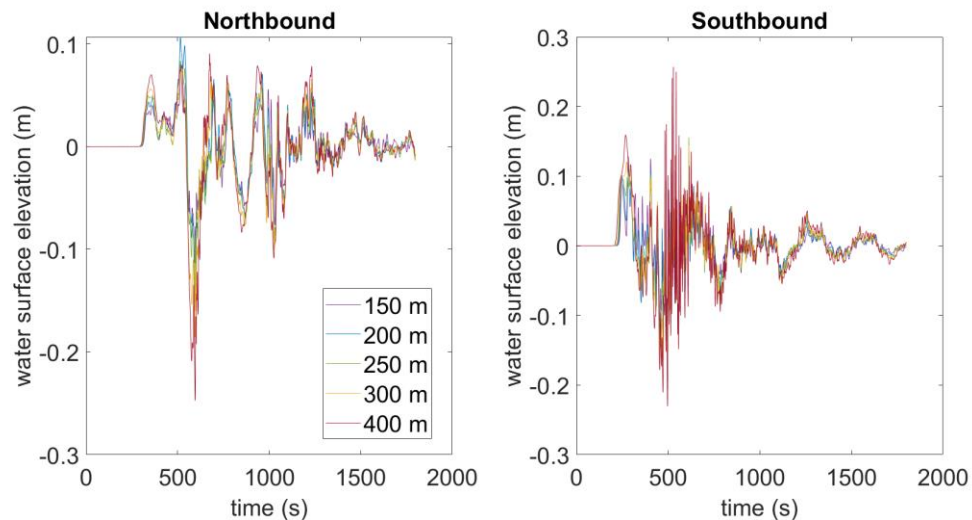


Figure 20. Time series results from vessel length test. Left panel shows northbound vessel wake simulation. Right panel shows southbound wake simulation.

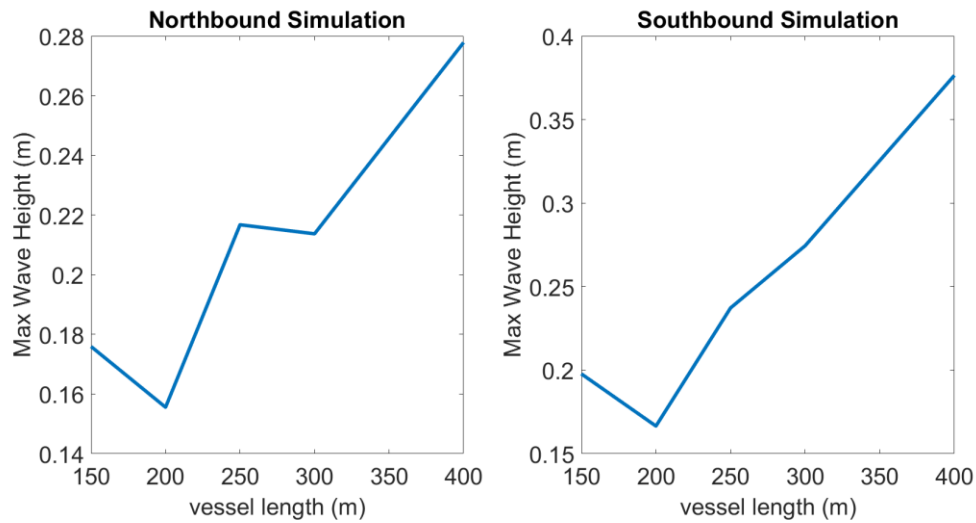


Figure 21. Comparison between vessel length and maximum modelled wave height. Maximum wave height was determined using a zero down-crossing algorithm.

While length had a weaker correlation with wave height than velocity, length is not an independent variable with respect to other ship parameters. Vessel capacity is correlated strongly with both vessel length and draft (Park et al. 2019). As vessels continue to grow larger, length *and* draft increase, especially given that beam size is limited by port and channel sizes. As such, vessel draft is also a worthy parameter to test to evaluate the impact of increasing vessel capacity.

#### 4.3.4 Vessel Draft

Validation has already demonstrated the substantial effect draft can have on simulation results. The drafts of validated cases ranged from 4.5 m to 10.5 m. As such, model simulations were performed with drafts of 4.5, 6.5, 8.5, and 10.5 m (Figure 22). There is a clear positive correlation between vessel draft and maximum wave height.

Over the validated parameter space of draft, maximum wave height more than doubles from minimum to maximum drafts (Figure 23).

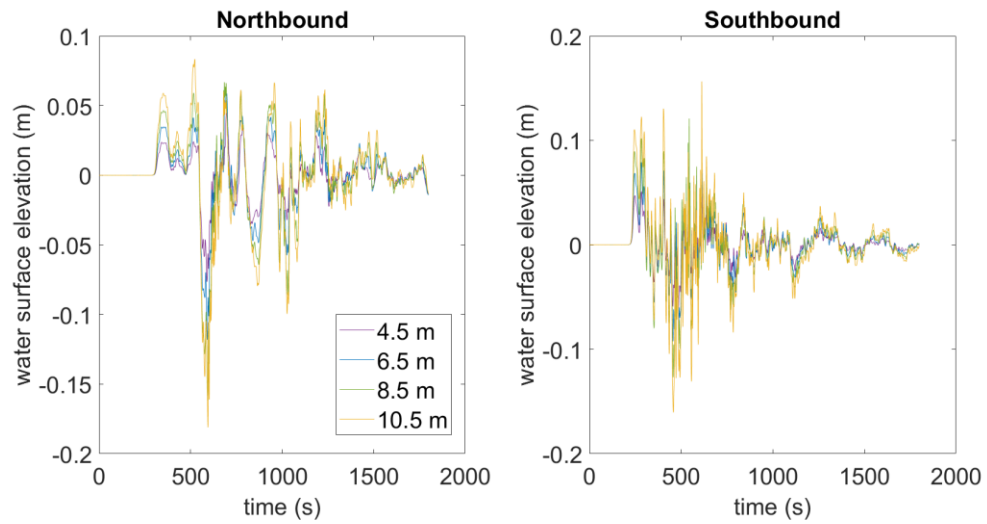


Figure 22. Time series results from vessel draft test. Left panel shows northbound vessel wake simulation. Right panel shows southbound wake simulation.

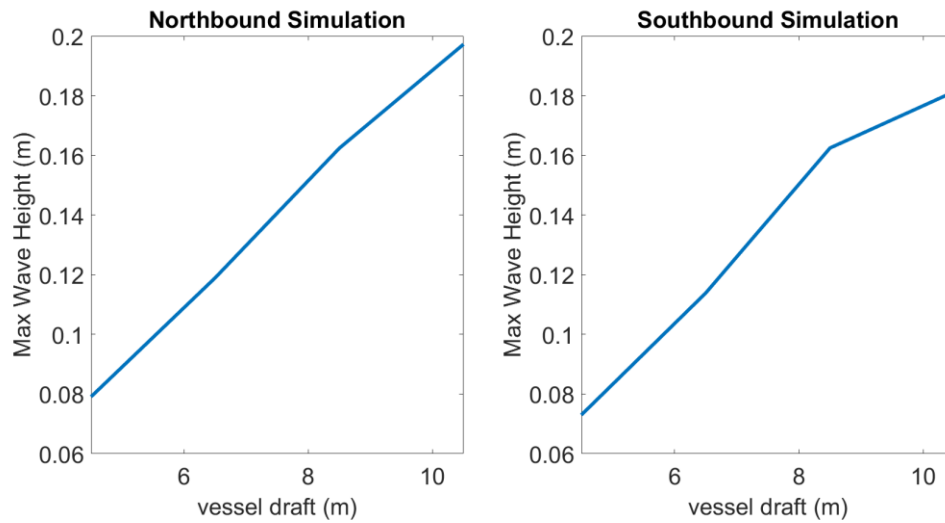


Figure 23. Comparison between vessel draft and maximum modelled wave height. Maximum wave height was determined using a zero down-crossing algorithm.

#### 4.3.5 Water Level

Water level tests were performed to determine when the wake environment is most energetic. Water level is a complicated factor, because it simultaneously affects the generation of wake in the channel as well as the shoaling and breaking of waves on the shore. The same water levels were tested as in the tests with and without the structure. Results from this test showed a limited effect of water level on maximum wave height (Figure 24). Both northbound and southbound simulations had a maximum wave height range of less than 0.1 m. There is also less of a positive trend than with the vessel-based parameters (Figure 25). Both show a peak maximum wave height in the mid tidal range. The optimum water level is likely the highest water level at which the breaking criterion is not reached, allowing maximum wave shoaling without dissipation via breaking.

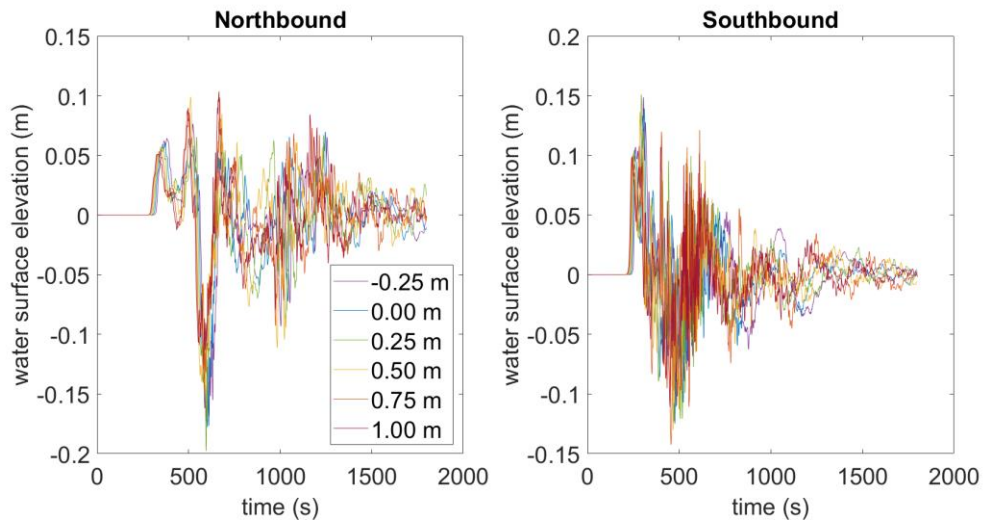


Figure 24. Time series results from water level test. Left panel shows northbound vessel wake simulation. Right panel shows southbound wake simulation.

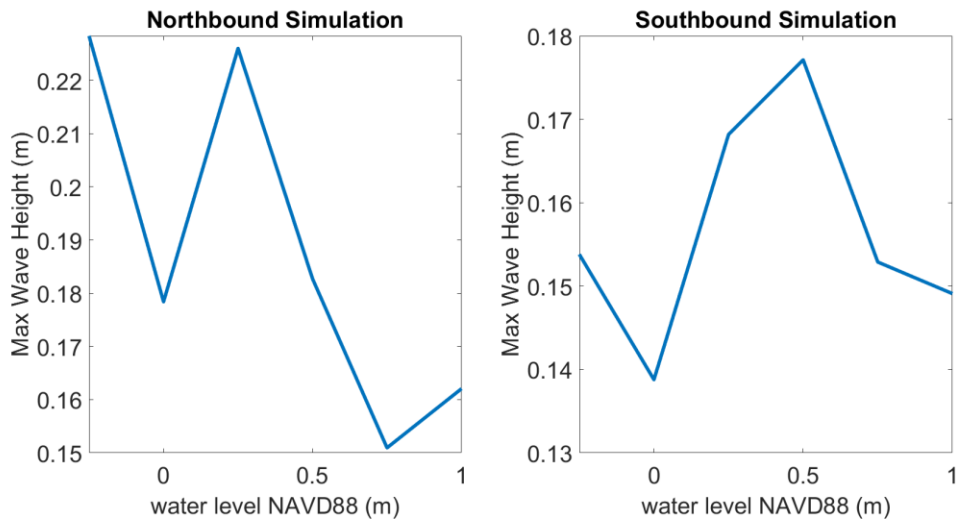


Figure 25. Comparison between water level and maximum modelled wave height. Maximum wave height was determined using a zero down-crossing algorithm.

## Chapter 5

### CONCLUSIONS AND FUTURE WORK

Parametric studies were conducted to determine variability in vessel wake. Vessel speed was the single most influential factor affecting maximum wave height. Within the range of velocities from the 20 validated cases (4.19 – 7.20 m/s), maximum wave height quadruples. This conclusion could motivate research on the implications of further limiting commercial vessel speed in estuarine waterways or near sites of designated environmental importance. Vessel draft and length have similar relationships to maximum wave height, suggesting that the growing size of the global vessel fleet may indicate a corresponding increase in vessel wake intensity. As such, subsequent numerical model simulations should combine the effect of increased vessel length and draft to compare the effects of velocity with the comprehensive effects of vessel size on the wake environment. Future work could also be undertaken to investigate the importance of channel depth on the wake environment, especially given the recent deepening of the Delaware River.

The model validation was relatively successful, with some variation based on ship heading. Northbound vessel simulations were performed with less than 15% drawdown error in eight out of ten simulations performed, while southbound vessel simulations were performed with less than 15% drawdown error only two times of the ten simulations performed. Northbound wake simulations may have been more successful because initial shape parameter calibration was completed using only a northbound wake signal. The northbound vessel wake signals contained smaller amplitude Kelvin wake in comparison to southbound vessel wake signals. There may also be unresolved features in the bathymetry only affecting the propagation of

southbound or northbound vessel wakes. A more accurate bathymetry could be used to continue investigation of this hypothesis. Further validation attempts can use more precise  $\alpha$  and  $\beta$  parameters, as well as draft measurements, to determine if the validated simulated cases match the actual measured drafts of passing vessels. Future validation efforts should include velocity data in service of validation of the sediment transport module.

Results of this investigation with regards to living shorelines are clear. Sisal twine is not a living shoreline material suited for medium-to-high energy environments. Coir logs may be suitable for these environments, provided they are properly secured with piles and tension lines capable of withstanding wake and storm forces. Model results indicated that the structure itself did effectively attenuate wake, particularly at low water levels. Up to a water level of 0.25 m, which covers more than half of the tidal range of the site, the structure reduced energy flux near the shore by 40%. This effect is even greater at lower water levels. Future work could be done to investigate the ideal placement of the structure in the cross-shore direction to maximize performance over the entire tidal range.

## REFERENCES

- Albers, Thorsten. (2018). The T-fence story – application of permeable bamboo fences in the Lower Mekong Delta, Vietnam. Retrieved from <http://coastal-protection-mekongdelta.com/download/Tools/TOOLS%20CPMD%20The%20T-fence%20story.pdf>
- Asplund, T. R., & Cook, C. M. (1997). Effects of motor boats on submerged aquatic macrophytes. *Lake and Reservoir Management*, 13(1), 1–12. <https://doi.org/10.1080/07438149709354290>
- Bhowmik, N. G. (1975). ABoat-generated waves in lakes@ Technical Note, Journal of the Hydraulics Division, American Society of Civil Engineers, November, 1465-68.
- Bhowmik, N. G., Soong, T. W., Reichelt, W. F., and Seddik, N. M. L. (1991). Waves generated by recreational traffic on the Upper Mississippi River system, Research Report 117, Department of Energy and Natural Resources, Illinois State Water Survey, Champaign, IL.
- Bilkovic, D. M., Mitchell, M. M., Davis, J., Herman, J., Andrews, E., King, A., Mason, P., Tahvildari, N., Davis, J., & Dixon, R. L. (2019). Defining boat wake impacts on shoreline stability toward management and Policy Solutions. *Ocean & Coastal Management*, 182, 104945. <https://doi.org/10.1016/j.ocecoaman.2019.104945>
- Brady, John. Delaware River Main Channel Deepening Project Supplemental Environmental Impact Statement. USACE, Philadelphia District. July 1997. <https://www.nap.usace.army.mil/Portals/39/docs/Civil/Deepening/Environmental/Abstract,%20table%20of%20contents,%20summary,%20Purpose%20and%20Need%20for%20Action.pdf> Accessed June 2022.
- Center for Advanced Infrastructure and Transportation (CAIT). (2012). Modeling and Analysis of the Vessel Traffic in the Delaware River and Bay Area Risk Assessment and Mitigation. Piscataway, NJ: Rutgers, The State University of New Jersey. Retrieved from: [https://cait.rutgers.edu/wp-content/uploads/2018/05/204-ru6532\\_0.pdf](https://cait.rutgers.edu/wp-content/uploads/2018/05/204-ru6532_0.pdf)
- Cowart, L., Walsh, J. P., & Corbett, D. R. (2010). Analyzing estuarine shoreline change: A case study of cedar island, North Carolina. *Journal of Coastal Research*, 265, 817–830. <https://doi.org/10.2112/jcoastres-d-09-00117.1>
- Clarksons. (2011). Containership Register. London, UK. [https://www.crs1.com/samples/LINER\\_Sample.pdf](https://www.crs1.com/samples/LINER_Sample.pdf). Accessed July 2022.

- Currin, C. A., Delano, P. C., Lexia, A., Valdes-Weaver, M., Currin, C. A., Delano, P. C., et al. (2008). Utilization of a citizen monitoring protocol to assess the structure and function of natural and stabilized fringing salt marshes in North Carolina. *Wetl. Ecol. Manag.* 16, 97–118. doi: 10.1007/s11273-007- 9059-1
- El Safty, H., & Marsooli, R. (2020). Ship Wakes and Their Potential Impacts on Salt Marshes in Jamaica Bay, New York. *Journal of Marine Science and Engineering*, 8(5), 325. <https://doi.org/10.3390/jmse8050325>
- Ertekin, R.C., Webster, W.C., Wehausen, J.V. (1986). Waves caused by a moving disturbance in a shallow channel of finite width. Cambridge University Press, 169: 275-292. DOI: 10.1017/S0022112086000630
- Gabel, F., Lorenz, S., & Stoll, S. (2017). Effects of ship-induced waves on aquatic ecosystems. *Science of The Total Environment*, 601-602, 926–939. <https://doi.org/10.1016/j.scitotenv.2017.05.206>
- Gourlay, T. (2001). The supercritical bore produced by a high-speed ship in a channel. *Journal of Fluid Mechanics*, 434, 399-409. doi:10.1017/S002211200100372X
- Herbert, D., Astrom, E., Bersosa, A., Batzer, A., McGovern, P., Angelini, C., Wasman, S., Dix, N., & Sheremet, A. (2018). Mitigating Erosional Effects Induced by Boat Wakes with Living Shorelines. *Sustainability*, 10(2), 436. <https://doi.org/10.3390/su10020436>
- Liu, Y., & Deng, R. (2018). Ship Wakes in Optical Images. *Journal of Atmospheric and Oceanic Technology*, 35(8), 1633–1648. <https://doi.org/10.1175/jtech-d-18-0021.1>
- Morris, R.L., Konlechner, T.M., Ghisalberti, M., Swearer, S.E. (2018). From grey to green: efficacy of eco-engineering solutions for nature-based coastal defence. *Glob. Change Biol.* 24:1827-1842. National Research Council. (2007) *Mitigating Shore Erosion on Sheltered Coasts*. Washington, D.C.: National Academies, 208p.
- Ng, Michelle. (2011). Vessel Wake Study. Moffat & Nichol. Project No. 7333. Retrieved June 12, 2022.
- O'Donnell, J. E.D. (2017). Living Shorelines: A Review of Literature Relevant to New England Coasts. *Journal of Coastal Research*, 33(2), 435-451.
- Park NK, Suh SC. (2019) Tendency toward Mega Containerships and the Constraints of Container Terminals. *Journal of Marine Science and Engineering*. 7(5):131. <https://doi.org/10.3390/jmse7050131>

- Parnell, K. E., Soomere, T., Zaggia, L., Rodin, A., Lorenzetti, G., Rapaglia, J., & Scarpa, G. M. (2014, December 8). Ship-induced solitary Riemann waves of depression in Venice lagoon. *Physics Letters A*. Retrieved June 23, 2022, from <https://www.sciencedirect.com/science/article/pii/S0375960114012237>
- Parsons, Katharine C. "Heron Nesting at Pea Patch Island, Upper Delaware Bay, USA: Abundance and Reproductive Success." *Colonial Waterbirds*, vol. 18, no. 1, 1995, pp. 69–78. JSTOR, <https://doi.org/10.2307/1521400>. Accessed 16 Jun. 2022.
- Pijanowski, K. (2016) Patterns and Rates of Historical Shoreline Change in the Delaware Estuary [Master's thesis, University of Delaware]. ProQuest 10191317.
- Safak, I., Norby, P., Dix, N., Grizzle, R., Southwell, M., Veenstra, J., Acevedo, A., Cooper-Kolb, T., Massey, L., Sheremet, A., & Angelini, C. (2020). Coupling breakwalls with oyster restoration structures enhances living shoreline performance along energetic shorelines. *Ecological Engineering*, 158, 106071. <https://doi.org/10.1016/j.ecoleng.2020.106071>
- Safak, I., Angelini, C., & Sheremet, A. (2021). Boat wake effects on sediment transport in intertidal waterways. *Continental Shelf Research*, 222, 104422. <https://doi.org/10.1016/j.csr.2021.104422>
- Shi, F., Malej, M., Smith, J. M., & Kirby, J. T. (2018). Breaking of ship bores in a Boussinesq-type ship-wake model. *Coastal Engineering*, 132, 1–12.
- Shuster, R., Sherman, D. J., Lorang, M. S., Ellis, J. T., & Hopf, F. (2020). Erosive potential of recreational boat wakes. *Journal of Coastal Research*, 95(sp1), 1279. <https://doi.org/10.2112/si95-247.1>
- Smith, C.S., Rudd, M.E., Gittman, R.K., Melvin, E.C., Patterson, V.S., Renzi, J.J., Wellman, E.H., and Silliman, B.R. (2020) Coming to Terms With Living Shorelines: A Scoping Review of Novel Restoration Strategies for Shoreline Protection. *Front. Mar. Sci.* 7:434. Doi: 10.3389/fmars.2020.00434
- Smyth, A.R., Piehler, M.F. and Grabowski, J.H. (2015), Habitat context influences nitrogen removal by restored oyster reefs. *J Appl Ecol*, 52: 716-725. <https://doi.org/10.1111/1365-2664.12435>
- Sorenson, R. M. (1997). Prediction of Vessel-Generated Waves with Reference to Vessels Common to the Upper Mississippi River System. ENV Report 4. Lehigh University, Bethlehem, PA.

- Tran, Nguyen & Haasis, Hans. (2014). An empirical study of fleet expansion and growth of ship size in container liner shipping. *International Journal of Production Economics*. <http://doi.org/10.1016/j.ijpe.2014.09.016>
- Weggel, J. R., and Sorensen, R. M. (1986) Ship wave prediction for port and channel design. *Proceedings of the Ports '86 Conference, Oakland, CA, 19-21 May 1986*. Paul H. Sorensen, ed., American Society of Civil Engineers, New York, 797-814.
- Wu, T. Y.-T. (1987). Generation of upstream advancing solitons by moving disturbances. *Journal of Fluid Mechanics*, 184, 75–99.  
<https://doi.org/10.1017/s0022112087002817>
- Zabawa, C., and Ostrom, C. (1980). The role of boat wakes in shore erosion (in Anne Arundel County, Maryland), @ Final Report, Coastal Resources Division, Maryland Department of Natural Resources, Annapolis, MD.
- Zaggia, L., Lorenzetti, G., Manfé, G., Scarpa, G. M., Molinaroli, E., Parnell, K. E., Rapaglia, J. P., Gionta, M., & Soomere, T. (2017). Fast shoreline erosion induced by ship wakes in a coastal lagoon: Field evidence and remote sensing analysis. *PLOS ONE*, 12(10), e0187210.  
<https://doi.org/10.1371/journal.pone.0187210>

## Appendix

### PERMISSIONS

Parts of this work have also been published as the following:

Everett CL, Williams O, Ruggiero E, Larner M, Schaefer R, Malej M, Shi F, Bruck J, and Puleo JA (2022), Ship wake forcing and performance of a living shoreline segment on an estuarine shoreline. *Front. Built Environ.* 8:917945. doi: 10.3389/fbuil.2022.917945

Copyright information for Frontiers Built Environment is included below

(<https://www.frontiersin.org/guidelines/policies-and-publication-ethics/>):

## Policies and publication ethics

### Frontiers' policies

#### Open access and copyright

All Frontiers articles from July 2012 onwards are published with open access under the Creative Commons [CC-BY license](#) (the current version is CC-BY, version 4.0). This means that the author(s) retains copyright, but the content is free to download, distribute, and adapt for commercial or non-commercial purposes, given appropriate attribution to the original article.

Upon submission, the author(s) grants Frontiers a license to publish, including to display, store, copy, and reuse the content. The CC-BY Creative Commons attribution license enables anyone to use the publication freely, given appropriate attribution to the author(s) and citing Frontiers as the original publisher. The CC-BY Creative Commons attribution license does not apply to third-party materials that display a copyright notice to prohibit copying. Unless the third-party content is also subject to a CC-BY Creative Commons attribution license, or an equally permissive license, the author(s) must comply with any third-party copyright notices.